Int. J. Solids Structures, 1971, Vol. 7, pp. 1539 to 1553. Pergamon Press. Printed in Great Britain

DEFORMATION OF AN INERTIA-LOADED THIN RING IN A RIGID CAVITY WITH INITIAL CLEARANCE

R. D. McGHIE

San Diego State College, San Diego, California

and

D. O. BRUSH

University of California, Davis, California

Abstract—The deformation of a thin circular ring of uniform thickness contained in a rigid circular cavity with small initial clearance between the ring and cavity is considered. The displacement of the ring produced by an acceleration of the rigid cavity in the plane of the ring is analyzed using nonlinear bending theory. Steady state acceleration only is considered so that the inertia forces can be treated as static loads. Variables considered are initial clearance, ring thickness and acceleration magnitude. The friction between the ring and cavity is assumed to be zero. A closed-form solution to the linear portion of the governing differential equations is given. A numerical solution is obtained to the nonlinear differential equations, and a particular ring-cavity geometry is studied using this numerical solution. Results are compared with a ring-cavity system having zero clearance. The comparison shows the effects of clearance on the ring-cavity system and indicates the sharp reduction in critical load due to small initial radial clearance.

INTRODUCTION

RECENT studies by Zagustin and Herrmann [1] and Pian and Bucciarelli [2] treated the buckling of a radially constrained circular ring subjected to in-plane inertia loading, when there is no initial clearance between the ring and the enclosing structure. The present investigation specifically examines the influence of a small radial clearance between ring and enclosure. The distinction can be of significance in the analysis of constrained cylindrical structures subjected to sudden lateral displacement.

The deformation of a thin circular ring of uniform thickness contained in a rigid circular cavity is considered. The displacement of the ring produced by an acceleration of the rigid cavity in the plane of the ring is analyzed. Steady state acceleration is considered, and the inertia forces are treated as static loads. In the initially undeformed state the ring has one point of contact with the cavity. When the system is accelerated, the ring deforms and a segment of the ring comes into contact with the cavity as shown in Fig. 1. As the loading is increased, the length of this contact segment increases until a critical value of the load is reached and the ring collapses.

The system is analyzed by use of nonlinear bending theory for the ring deformation. Variables considered are initial clearance between ring and cavity, ring thickness and acceleration magnitude. The friction between the ring and cavity is assumed to be zero, and the ring material is assumed to remain elastic.

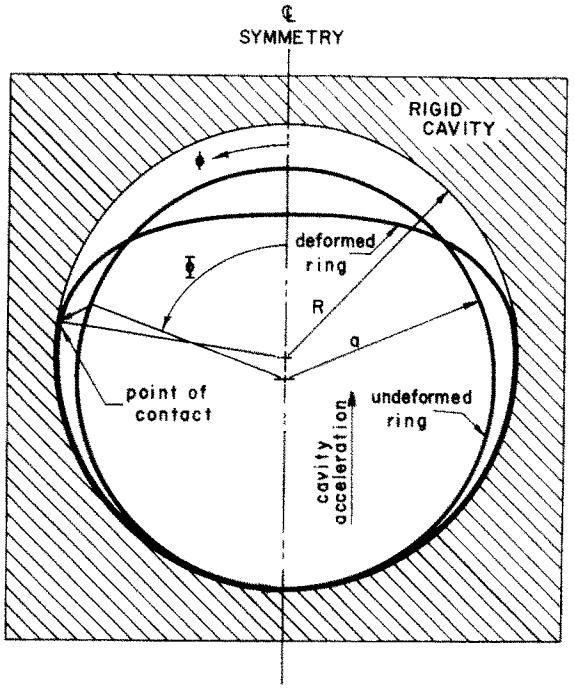

FIG. 1. Schematic of ring-cavity.

ANALYSIS

The analysis of the system is carried out by use of a semi-inverse method. An angle to contact Φ (Fig. 1) is specified and the nondimensional inertia load factor γ which would cause the system to have this angle to contact is sought. This approach permits the ring to be separated into two segments, an upper segment which is independent of the cavity constraint, and a lower segment which is constrained by the cavity. The solution for the system is achieved by enforcement of the appropriate compatibility relations at the point of contact Φ.

The lower ring segment is treated as a circular arch subjected to steady state acceleration and constrained by the rigid cavity in such a way that its radius in the deformed shape is equal to that of the cavity. The upper ring segment is considered to be subjected to the same steady state accleration, but to be constrained only at its terminal points by the lower ring segment.

The governing nonlinear differential equations are applicable to what Novozhilov [3] has called "intermediate" bending of thin rings. Their formulation is carried out by deriving strain–displacement relations for small strains and moderately-small rotations, and relating the strain at any point in the ring to centroidal-surface displacement components by use of the Kirchhoff approximations. Constitutive relations are based on Hooke's law. Equilibrium equations are derived by summation of forces and moments on a ring element in a slightly deformed configuration. The kinematic relations, constitutive relations and equilibrium equations are combined to yield a set of two nonlinear ordinary differential equations in terms of displacement components and load.

Assumptions made in the analysis are the following:

1. The ring deforms symmetrically with respect to the vertical axis.
2. There is no friction between ring and cavity.
3. The thickness–radius ratio (h/a) of the ring is much smaller than unity.
4. The hoop strains ε and rotations ω are much less than unity.
5. The cavity material is rigid and the ring material behaves elastically.
6. The loading is static, i.e. not a function of time.
7. The ring has a rectangular cross-section (and is of unit width).

KINEMATIC RELATIONS

Let r and ϕ denote the radial and circumferential coordinates of an arbitrary point in the undeformed ring, $\bar{v}, \bar{w}$ the tangential and radial displacement components of that point, and $\bar{\varepsilon}$ the extensional strain of a circumferential line element. For $\bar{\varepsilon}$ small compared with unity the relation between strain and displacements is readily shown to be (e.g. Ref. [4], equation (14)):

$$\bar{\varepsilon} = \left(\frac{\bar{v}' - \bar{w}}{r}\right) + \frac{1}{2}\left(\frac{\bar{v}' - \bar{w}}{r}\right)^2 + \frac{1}{2}\left(\frac{\bar{v} + \bar{w}'}{r}\right)^2 \tag{1}$$

where primes denote differentiation with respect to ϕ.

For moderately small rotations, from Fig. 2,

$$\bar{\omega} = \frac{\bar{v} + \bar{w}'}{r}. \tag{2}$$

For both $\bar{\varepsilon}$ and $\bar{\omega}$ small compared with unity, the first quadratic term in equation (1) may be neglected (we exclude from consideration cases in which $\bar{v}'$ or $\bar{w}$ are of the magnitude of the radius r or larger) and that equation simplified to the form:

$$\bar{\varepsilon} = \left(\frac{\bar{v}' - \bar{w}}{r}\right) + \frac{1}{2}\left(\frac{\bar{v} + \bar{w}'}{r}\right)^2. \tag{3}$$

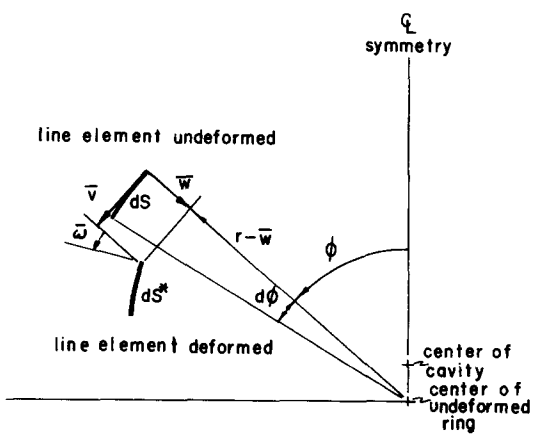

FIG. 2. Circumferential line element in ring.

Ring bending theory is based on the simplifying approximation that normals to the undeformed centroidal surface remain straight, normal and inextensional during the deformation. Therefore, from Fig. 3, displacement components $\bar{v}, \bar{w}$ may be expressed in terms of the corresponding displacements v, w of a point on the centroidal surface by the relations:

$$\begin{aligned} \bar{v} &= v - z\omega \\ \bar{w} &= w \end{aligned} \tag{4}$$

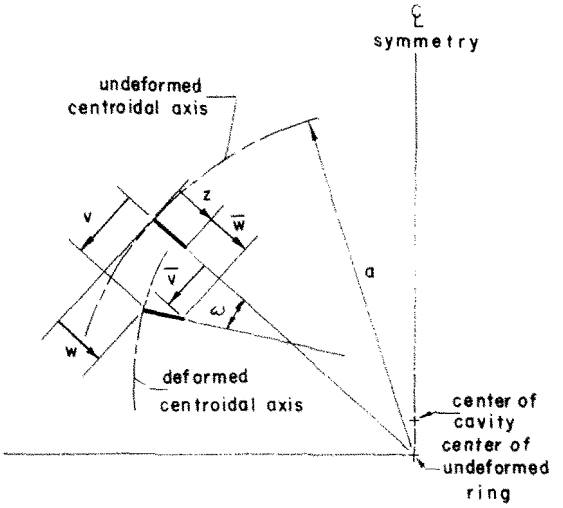

FIG. 3. Normal to ring centroidal surface.

where ω represents rotation at a point on the centroidal surface and is small compared with unity. From equation (2),

$$\omega = \frac{v + w'}{a}. \tag{5}$$

Introduction into equation (3), rearrangement and observation that $r \approx a$ for a thin ring give

$$\bar{\varepsilon} = \frac{v' - w}{a} + \frac{1}{2}\omega^2 - z\frac{\omega'}{a}. \tag{6}$$

[It may be seen from equations (2), (4) and (5) that $\omega = \bar{\omega}$.]

The extensional strain ε of a circumferential line element on the centroidal surface is obtained by setting $z = 0$ in equation (6). The curvature change κ of a centroidal line element may be defined as the rate of change of the rotation ω in the circumferential direction. Therefore, equation (6) can be written

$$\bar{\varepsilon} = \varepsilon - z\kappa \tag{7}$$

where

$$\varepsilon = \left(\frac{v' - w}{a}\right) + \frac{1}{2}\left(\frac{v + w'}{a}\right)^2, \tag{8}$$

and

$$\kappa = \frac{v' + w''}{a^2}. \tag{9}$$

The κ is positive when the radius at a point on the centroidal surface decreases.

CONSTITUTIVE EQUATIONS

For an elastic material the relation between the stress $\bar{\sigma}$ and strain $\bar{\varepsilon}$ is expressed through Hooke's law as

$$\bar{\sigma} = E\bar{\varepsilon} \tag{10}$$

where the constant E represents Young's modulus. Definition of the stress resultant N and the moment M in the usual manner leads to the relations

$$N = EA\varepsilon, \qquad M = -EI\kappa \tag{11}$$

where I is the cross-sectional moment of inertia. With the sign convention used here, a positive moment causes an increase in radius.

On substituting the relations for ε and κ into equation (11) the values for $N(\phi)$ and $M(\phi)$ can be expressed in terms of centroidal-surface displacement components as follows:

$$N(\phi) = EA\left[\left(\frac{v' - w}{a}\right) + \frac{1}{2}\left(\frac{v + w'}{a}\right)^2\right] \tag{12}$$

and

$$M(\phi) = -EI\left(\frac{v' + w''}{a^2}\right). \tag{13}$$

GOVERNING EQUILIBRIUM EQUATIONS

The governing nonlinear differential equations of equilibrium are derived by applying the equations $\sum F = \sum M = 0$ to an element of the deformed ring. The ring element is in a state of equilibrium under the action of external loads and internal forces, as shown in Fig. 4. The equations are expressed in terms of the undeformed coordinate system, and simplifying approximations are made in these equations which are consistent with the assumptions of small elongations and moderately small rotations.

Since steady state acceleration is considered here, the inertia forces may be treated as static loads. Thus the loading dP on the ring element can be expressed in terms of the undeformed geometry as

$$dP = \gamma\rho A\, dS = \gamma\rho Aa\, d\phi \tag{14}$$

where ρ, A and dS are weight density, area and element length of the undeformed element.

The force $p(\phi)\, dS^*$ is the foundation reaction and acts only in the range $\Phi \leq \phi \leq \pi$.

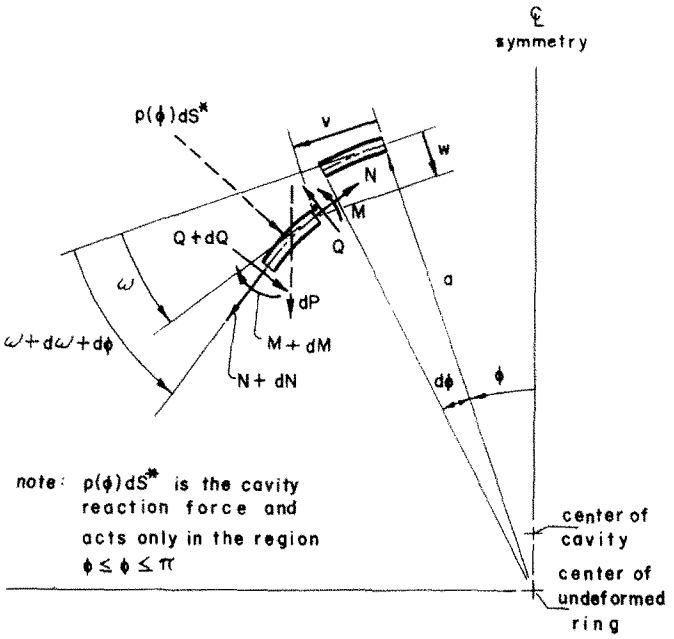

FIG. 4. Ring element in equilibrium.

Summation of forces in the tangential and normal directions and summation of the moments yield the following three equations of equilibrium:

$$N' - N\omega - Q - pa\omega\left[1 + \left(\frac{v' - w}{a}\right)\right] + \gamma\rho Aa \sin\phi = 0 \tag{15}$$

$$(N\omega)' + N + Q' + pa\left[1 + \left(\frac{v' - w}{a}\right)\right] + \gamma\rho Aa \cos\phi = 0 \tag{16}$$

$$M' - Qa = 0 \tag{17}$$

where N, M and Q are centroidal hoop force, bending moment and tranverse shear force, respectively. In these equations $\sin\omega$ and $\cos\omega$ are replaced by ω and unity, respectively, and quadratic terms representing products of the small quantities Q and ω or Q and ε are neglected. The latter approximation is consistent with those utilized in the derivation of the kinematic relations, i.e. that normals to the centroidal surface remain straight and normal during the deformation. Such terms are missing from the outset when the equilibrium equations are derived variationally from a potential energy expression in which the strain energy due to transverse shearing strains is neglected (Ref. [5]).

Elimination of Q from equations (15) and (16) by use of equation (17) yields:

$$N' - N\omega - \frac{1}{a}M' - pa\omega + \gamma\rho Aa \sin\phi = 0 \tag{18}$$

and

$$N + (N\omega)' + \frac{1}{a}M'' + p(a + v' - w) + \gamma\rho Aa \cos\phi = 0 \tag{19}$$

where cubic terms (but not quadratic terms) representing products of the small quantities p, ω and $(v' - w)/a$ have been neglected. Transformation of the above equations into functions of displacement components yields the following two nonlinear differential equations:

$$a(v''-w')+(v+w')(v'+w'')-(v'-w)(v+w')-\frac{1}{2a}(v+w')^3+ka(v''+w''')$$

$$-\frac{pa^2}{EA}(v+w')+\frac{\gamma\rho a^3}{E}\sin\phi=0 \tag{20}$$

and

$$(v''-w')(v+w')+\frac{3}{2a}(v+w')^2(v'+w'')+(v'-w)(v'+w'')+a(v'-w)+\tfrac{1}{2}(v+w')^2$$

$$-ka(v'''+w'''')+\frac{pa^2}{EA}(a+v'-w)+\frac{\gamma\rho a^3}{E}\cos\phi=0, \tag{21}$$

where $k = I/(a^2A)$.

Equations (20) and (21) are the governing equilibrium equations in terms of the displacement components v, w, the foundation reaction p and the load factor γ. The same equations also have been derived on the basis of stationary potential energy theory in Ref. [5].

UPPER RING SEGMENT

The upper ring segment consists of that portion of the ring not in contact with the cavity, i.e. the part in the region $0 \leq \phi < \Phi$. The two governing differential equations are, from equations (20) and (21),

$$kw'''-w'+(1+k)v''+\frac{\gamma\rho a^2}{E}\sin\phi=P1 \tag{22}$$

and

$$kw''''+w+kv'''-v'-\frac{\gamma\rho a^2}{E}\cos\phi=P2 \tag{23}$$

where $P1$ and $P2$ represent the nonlinear terms in the respective equations and are given by:

$$P1=-\frac{1}{a}(v+w')(w+w'')+\frac{1}{2a^2}(v+w')^3 \tag{24}$$

and

$$P2=\frac{1}{a}(v''-w')(v+w')+\frac{1}{a}(v'-w)(v'+w'')+\frac{1}{2a}(v+w')^2\left[1+\frac{3}{a}(v'+w'')\right]. \tag{25}$$

The boundary conditions at the top centerline, $\phi = 0$, are, from symmetry,

$$v=w'=v''+w'''=0. \tag{26}$$

At the point of contact, $\phi = \Phi$, the displacement components (kinematic boundary conditions) for v, w and w' must be matched to those of the lower ring segment. Supplemental conditions to be fulfilled at this point are that the internal forces N and M (static boundary conditions) must be compatible with those of the lower ring segment. In Ref. [5] the same kinematic and static boundary conditions for the upper ring segment were obtained variationally.

Having found v and w, the internal hoop force, moment and shear can be found by using the constitutive relations, equations (12) and (13), and the equilibrium equation (17), i.e.

$$N(\phi) = EA\left[\left(\frac{v'-w}{a}\right)+\frac{1}{2}\left(\frac{v+w'}{a}\right)^2\right] \tag{27}$$

$$M(\phi) = -EI\left(\frac{v'+w''}{a^2}\right) \tag{28}$$

and

$$Q(\phi) = -EI\left(\frac{v''+w'''}{a^3}\right). \tag{29}$$

LOWER RING SEGMENT

The lower ring segment consists of that portion of the ring in contact with the cavity, i.e. that part in the region $\Phi \le \phi \le \pi$. The two differential equations to be satisfied in order to describe the forces in this ring segment are, from equations (18) and (19),

$$N' - N\omega - \frac{1}{a}M' - pa\omega + \gamma\rho Aa\sin\phi = 0 \tag{30}$$

$$N + (N\omega)' + \frac{1}{a}M'' + p(a+v'-w) + \gamma\rho Aa\cos\phi = 0. \tag{31}$$

They differ from those for the upper ring segment in that they contain the cavity reaction force $p(\phi)$.

In this segment of the ring both the deformed and undeformed shape are known. This allows for some basic kinematic relations to be derived. An exact relation for ε in terms of rotation ω is developed using Fig. 5 to give

$$\varepsilon = \frac{R}{a}\omega' + \frac{f}{a} \tag{32}$$

where $f = R - a$. Exact relations for v and w in terms of rotation ω are, from Fig. 5,

$$v = R\sin\omega - f\sin\phi \tag{33}$$

and

$$w = a - R\cos\omega - f\cos\phi. \tag{34}$$

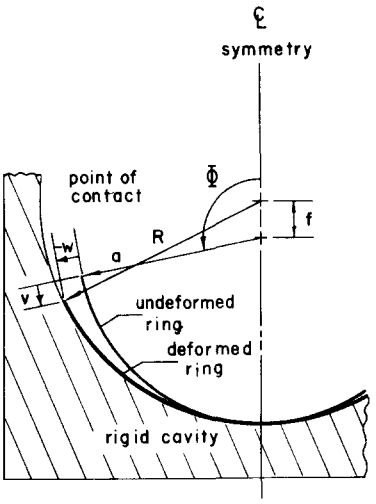

FIG. 5. Lower ring segment geometry.

The change in curvature κ is known in terms of the undeformed radius a and the deformed radius R, i.e.

$$\kappa = \frac{1}{R} - \frac{1}{a} = -\frac{f}{aR}. \tag{35}$$

Combining equation (35) with (11) gives for the bending moment in the lower ring segment the expression

$$M = \frac{EIf}{aR}. \tag{36}$$

On substituting equation (36) into (17) the shear force Q of course is found to be $Q = 0$.

The principal interest of this problem lies in the case in which the original ring clearance is small compared with the radius. Hence, the lower ring segment has relatively small rotations, and its analysis may be satisfactorily treated as linear. Thus from equations (30) and (31) the two governing linear differential equations become

$$N' + \gamma\rho Aa \sin\phi = 0 \tag{37}$$

$$N + pa + \gamma\rho Aa \cos\phi = 0. \tag{38}$$

On recalling that $N = EA\varepsilon$, the differential equations may be written

$$\varepsilon' + \frac{\gamma\rho a}{E} \sin\phi = 0 \tag{39}$$

$$\varepsilon + \frac{pa}{EA} + \frac{\gamma\rho a}{E} \cos\phi = 0. \tag{40}$$

Equations (32) and (39) yield a second order differential equation for the rotation.

$$\omega'' = -\frac{\gamma\rho a^2}{E}\frac{\sin\phi}{R} \tag{41}$$

Integration of this equation twice gives an expression for ω in terms of two integration constants D_1 and D_2:

$$\omega' = \frac{\gamma\rho a^2}{E}\frac{\cos\phi}{R} + D_1 \tag{42}$$

and

$$\omega = \frac{\gamma\rho a^2}{E}\frac{\sin\phi}{R} + D_1\phi + D_2. \tag{43}$$

At $\phi = \pi$, $\omega(\pi) = 0$ from symmetry, so that $D_2 = -D_1\pi$, and the rotation in the lower ring segment is

$$\omega(\phi) = \frac{\gamma\rho a^2}{E}\frac{\sin\phi}{R} + D(\phi - \pi), \tag{44}$$

where D has been used in place of D_1. From equations (44) and (32),

$$\varepsilon = \frac{\gamma\rho a}{E}\cos\phi + \frac{RD}{a} + \frac{f}{a}. \tag{45}$$

From equations (40) and (45) the foundation reaction force is

$$\frac{pa}{EA} = -2\frac{\gamma\rho a}{E}\cos\phi - \frac{RD}{a} - \frac{f}{a}. \tag{46}$$

Using equation (45) the hoop force is

$$\frac{N}{EA} = \frac{\gamma\rho a}{E}\cos\phi + \frac{RD}{a} + \frac{f}{a}. \tag{47}$$

The expressions for v and w in equations (33) and (34) give

$$v = R\omega - f\sin\phi \tag{48}$$

and

$$w = -f(1 + \cos\phi). \tag{49}$$

Substitution of equations (44) into (48) gives v in terms of γ and D:

$$v = \frac{\gamma\rho a^2}{E}\sin\phi + RD(\phi - \pi) - f\sin\phi. \tag{50}$$

In summary, the lower ring segment can be described in terms of the load factor γ and a constant D (which must be evaluated in combination with the upper ring segment) by equations (36), (44), (46), (47), (49) and (50).

LINEAR CLOSED-FORM SOLUTION

A linear closed-form analysis for the overall system is made by linearizing the governing differential equations for the upper ring segment and combining the solution of these linearized equations with that for the equations governing the lower ring segment.

On neglecting the nonlinear terms in equations (22) and (23) a set of linear non-homogeneous equations is obtained for the upper ring segment from which the variables can be uncoupled. The linearized differential equations are

$$kw''' - w' + (1+k)v'' = -\frac{\gamma\rho a^2}{E}\sin\phi \tag{51}$$

and

$$kw'''' + w + kv''' - v' = \frac{\gamma\rho a^2}{E}\cos\phi. \tag{52}$$

The solutions to these two equations are

$$w(\phi) = C_1 + C_2\sin\phi + C_3\cos\phi + C_4\phi\sin\phi + C_5\phi\cos\phi - \frac{\gamma\rho a^2}{E}\frac{(1+k)}{4k}\phi^2\cos\phi, \tag{53}$$

and

$$\begin{aligned} v(\phi) = {} & C_6 + C_1\phi - C_2\cos\phi + C_3\sin\phi \\ & + C_4\left[\left(\frac{1-k}{1+k}\right)\sin\phi - \phi\cos\phi\right] + C_5\left[\left(\frac{1-k}{1+k}\right)\cos\phi + \phi\sin\phi\right] \\ & + \frac{\gamma\rho a^2}{E}\left[\left(\frac{k-1}{2k}\right)\phi\cos\phi + \left(\frac{1+3k}{2k(1+k)}\right)\sin\phi - \left(\frac{1+k}{4k}\right)\phi^2\sin\phi\right] \end{aligned} \tag{54}$$

where the unknowns C_1, C_2, C_3, C_4, C_5 and C_6 are to be evaluated from the boundary conditions at $\phi = 0$ and $\phi = \Phi$.

Application of the boundary conditions at $\phi = 0$, i.e. $v = 0$, $w' = 0$ and $v'' + w''' = 0$ gives

$$C_2 = C_5 = C_6 = 0. \tag{55}$$

Satisfaction of the three displacement compatibility relations at $\phi = \Phi$, i.e. those on v, w and w', and the two force compatibility relations on N and M results in five non-homogeneous algebraic equations in the three unknown integration constants C_1, C_3, C_4 and the two unknowns from the lower ring segment, γ and D:

$$\begin{aligned} & C_1\Phi + C_3\sin\Phi + C_4\left[\left(\frac{1-k}{1+k}\right)\sin\Phi - \Phi\cos\Phi\right] \\ & + \frac{\gamma\rho a^2}{E}\left[\left(\frac{k-1}{2k}\right)\Phi\cos\Phi - \left(\frac{k+1}{4k}\right)\Phi^2\sin\Phi - \sin\Phi\right] + DR(\pi - \Phi) = -f\sin\Phi \end{aligned} \tag{56}$$

$$C_1 + C_3\cos\Phi + C_4\Phi\sin\Phi - \frac{\gamma\rho a^2}{E}\left(\frac{1+k}{4k}\right)\Phi^2\cos\Phi = -f(1+\cos\Phi) \tag{57}$$

$$C_3\sin\Phi - C_4(\Phi\cos\Phi + \sin\Phi) + \frac{\gamma\rho a^2}{E}\left(\frac{1+k}{4k}\right)(2\Phi\cos\Phi - \Phi^2\sin\Phi) = -f\sin\Phi \tag{58}$$

$$C_4\left(\frac{2k}{1+k}\right)\cos\Phi + \frac{\gamma\rho a^2}{E}\left[\Phi\sin\Phi + \frac{k-1}{2(1+k)}\cos\Phi\right] + DR = -f \tag{59}$$

and

$$C_1 + C_4\left(\frac{2}{1+k}\right)\cos\Phi + \frac{\gamma\rho a^2}{E}\left[\frac{1}{k}\Phi\sin\Phi + \left(\frac{k-1}{2k(1+k)}\right)\cos\Phi\right] = -\frac{af}{R}. \tag{60}$$

The simultaneous solution of these five equations yields values for the unknowns with which the displacement components and forces can be determined.

In Ref. [5] the linear analysis of the upper ring segment equations is carried out using the linearized form of the differential equations (18) and (19) to determine $N(\phi)$ and $M(\phi)$ and then using the linearized kinematic relations to find the displacement components v, w. The analysis yields complex but uncoupled expressions for N, M, v, w, γ and D as functions of Φ and ϕ.

NONLINEAR NUMERICAL SOLUTION

The linear closed-form solution for the lower ring segment is combined with a numerical nonlinear analysis of the upper ring segment to yield an overall solution to the deformation of the ring for moderately large deformations. The numerical analysis is carried out using a Newton–Raphson algorithm in conjunction with finite differences.

Transformation of the governing differential equations, equations (22) and (23), into a set of nonlinear algebraic equations is made using five-point central difference equations in the Lagrangian form [6]. Boundary conditions at the top centerline $\phi = 0$ are transformed using central difference equations and symmetry. Boundary (matching) conditions at the point of contact $\phi = \Phi$ are transformed using backward sloping difference equations and the linear closed-form solutions for displacement components from the lower ring segment solution. The two-point boundary value problem is thus transformed into a set of $2N+9$ nonlinear algebraic equations in $2N+9$ unknown quantities, where N is the number of pivotal points in the interval $[0, \Phi]$. A detailed account of the numerical analysis can be found in Ref. [5].

The set of equations, expressed in matrix notation, may be written as

$$Ax = B + P(x) \tag{61}$$

where A is a square matrix of the coefficients of the linear unknown terms, x is a column matrix of the unknown quantities (displacement components, loading function γ and constant D), B is a column matrix of known terms and $P(x)$ is a column matrix of the nonlinear terms in the unknown displacement components.

Prior to consideration of the nonlinear terms $P(x)$, an investigation of the accuracy of the computer solution to the set of linear equations

$$Ax = B \tag{62}$$

is made with regard to the effect of significant figures and the number of pivotal points used. Equation (62) is programmed in a machine code and a solution is obtained by an inversion of matrix A using a Gauss–Seidel iteration scheme. Calculations are carried out for a ring having a/h equal to 100 and an initial radial clearance f/a equal to 0·00143. Using this program, the angle to contact Φ is held constant, the number of pivotal points is varied, and the resulting solutions are compared with the linear closed-form results. A plot of the numerical results for the top centerline displacement and the inertial load factor γ vs. the number of pivotal points for $\Phi = 90°$ is shown in Fig. 6. This comparison indicates that it

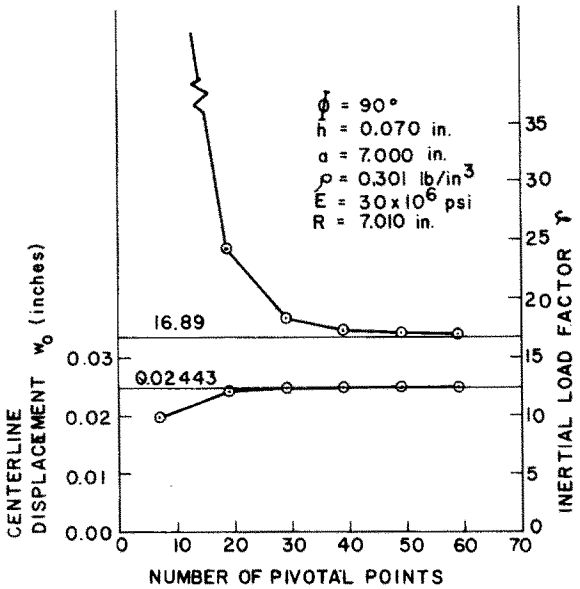

FIG. 6. Centerline displacement and inertial load factor vs. number of pivotal points.

is necessary to use double precision accuracy (14 significant figures) and to maintain a spacing between pivotal points equal to or less than 0·030 rad. in order to achieve numerical results to within 1 per cent of the linear closed-form solution.

The unusual accuracy required and the large number of pivotal points necessary to obtain a numerical solution to the equations are results of the highly coupled nature of the equations and of the ring-cavity geometry used. Complete coupling of the algebraic equations occurs through the inertial load factor γ, and the thickness parameter k in the numerical example has an order of magnitude of 10^{-7}.

For solution of the nonlinear problem represented by equation (61), the nonlinear difference equations are programmed in a machine code and a Newton–Raphson algorithm [7] is coded and used to solve the equations. This solution also is carried out for the ring having a/h equal to 100 and an initial radial clearance f/a equal to 0·00143.

For the necessary initial approximation to the solution to the difference equations, the linear values obtained from the numerical solution of equation (62), for a value of $\Phi = 50°$, are used. A nonlinear solution for this Φ is then obtained. A small increment of Φ is made and the starting values for the new Φ are the nonlinear values obtained for the previous Φ. This step-by-step procedure is repeated until the critical load is obtained. The size of the increment of Φ is governed by the number of iterations necessary to converge to within the desired accuracy. The algorithm gives an accuracy of convergence to within three significant figures.

RESULTS AND CONCLUSIONS

Results of the solution are shown in Figs. 7 and 8. In Fig. 7, a plot of load factor γ vs. top centerline displacement component w_0 is presented. Also shown for comparison is the result of the zero clearance solution given in Ref. [1]. This figure indicates that an initial

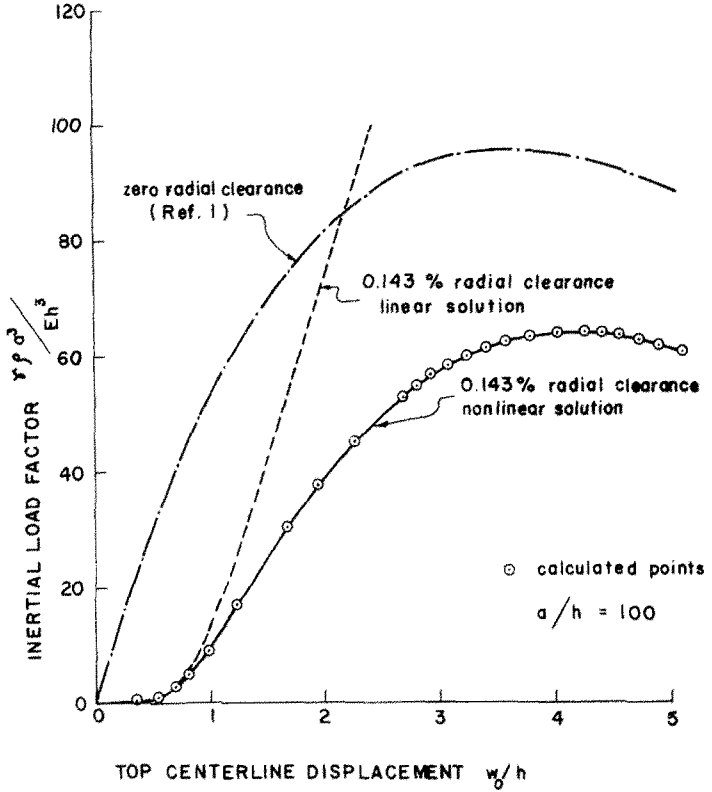

FIG. 7. Inertial load factor vs. top centerline displacement.

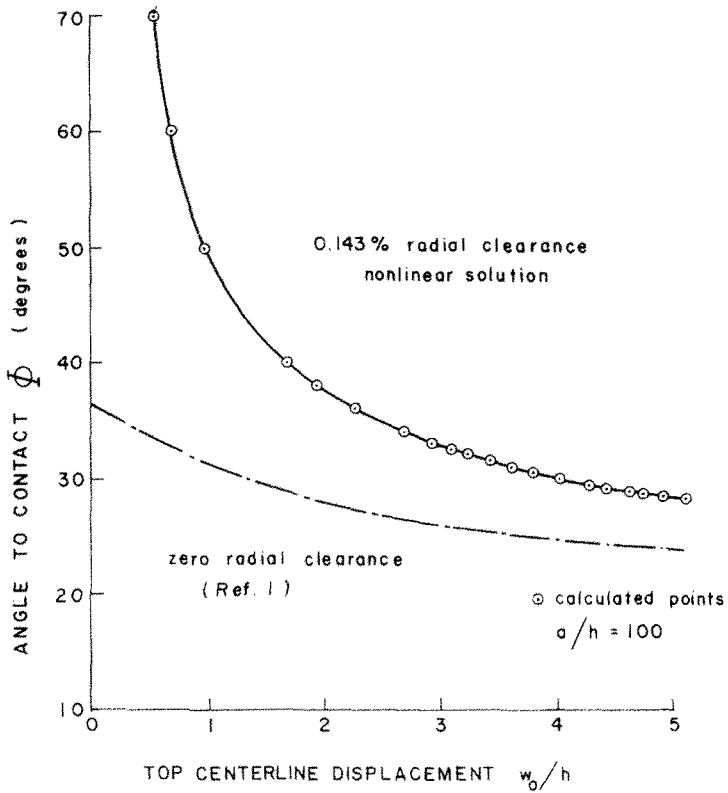

FIG. 8. Angle to contact vs. top centerline displacement.

radial clearance equal to 0·143 per cent of the initial ring radius causes a 33 per cent decrease in critical load relative to the zero-clearance case.

In Fig. 8, a plot of angle to contact Φ vs. top centerline displacement component w_0 is shown along with the above-mentioned zero clearance solution. This figure indicates that the critical load is reached before the minimum angle to contact is reached, and, as expected, that the initial clearance solution approaches the zero clearance solution for large values of w_0.

It is concluded that for such a ring-cavity system, a small initial radial clearance sharply reduces the critical load.

Acknowledgements—A portion of this work was sponsored by the Lawrence Radiation Laboratory at Livermore, California; the support of A. L. Austin is gratefully acknowledged. The authors also are indebted to S. R. Keim of the National Academy of Engineering's Committee on Ocean Engineering for suggestions which led to the initiation of the study.

REFERENCES

[1] E. A. ZAGUSTIN and G. HERRMANN, Stability of an elastic ring in a rigid cavity. *J. appl. Mech.* **89**, 263–270 (1967).
[2] T. H. H. PIAN and L. L. BUCCIARELLI, Buckling of radially constrained circular ring under distributed loading. *Int. J. Solids Struct.* **3**, 715–730 (1967).
[3] V. V. NOVOZHILOV, *Foundations of the Nonlinear Theory of Elasticity*. Graylock Press (1953).
[4] H. L. LANGHAAR, A. P. BORESI and D. R. CARVER, Energy Theory of Buckling of Circular Elastic Rings and Arches, *Proc. Second U.S. Nat. Congress Appl. Mech.*, pp. 437–443. ASME (1954).
[5] R. D. MCGHIE, Deformation of a Ring Contained in a Rigid Cavity, Ph.D. Thesis, University of California, Davis (1968).
[6] L. COLLATZ, *The Numerical Treatment of Differential Equations*. Springer-Verlag (1960).
[7] S. D. CONTE, *Elementary Numerical Analysis*. McGraw-Hill (1965).

(*Received* 17 *December* 1970; *revised* 22 *March* 1971)

Абстракт—Исследуется деформация тонкого, круглого кольца, постоянной толщины, находяеегося в жесткой круглой полости, с малым начальным зазором между кольцом и полостью. Используя нелинейную теорию изгиба, даётся анализ перемещения кольца, вызванного ускорением жесткой полости в плоскости кольца. Учитывается только стационарное ускорение так, что силы инерции можно рассматривать в смысле статической нагрузки. Расматриваемыми переменными являются:

начальный зазор, толщина кольца и величина ускорения. Предполагаетя нулевое трение между кольцом и полостью. Даётся решение в замкнутом виде, по отношении к линейной части определяющих дифференциальных уравнений. Исследуется подробно геометрия колца и полости, путём использования численного решения. Результаты сравниваются с системой кольца с нулевым зазором. Сравнение указывает эффекты зазора по отношении к системе кольцо-полрсть и значителвные уменшение критической нагрузки, вследствие малого начального радиального зазора.